

# A study of copper stoichiometry and phase relationships in the copper-zirconium phosphate system: $\text{CuZr}_2(\text{PO}_4)_3 - \text{Cu}_{0.5}\text{Zr}_2(\text{PO}_4)_3$

R. H.-W. CHRISTIANSEN, T. E. WARNER

*Department of Chemistry, University of Southern Denmark, Campusvej 55, DK-5230 Odense M, Denmark*

Published online: 4 February 2006

$\text{CuZr}_2(\text{PO}_4)_3$  crystallises with the Nasicon-type structure and is a copper(I) ion conductor. The possibility of a solid solution between  $\text{CuZr}_2(\text{PO}_4)_3$  and  $\text{Cu}_{0.5}\text{Zr}_2(\text{PO}_4)_3$  has been a controversial issue for many years. As part of a continued study,  $\text{CuZr}_2(\text{PO}_4)_3$  and  $\text{Cu}_{0.5}\text{Zr}_2(\text{PO}_4)_3$  were prepared by solid state methods and used to investigate the copper stoichiometry and phase relationships between these two materials as a function of copper content, temperature and oxygen fugacity. The following reversible reaction:  $\text{Cu}_{0.5}\text{Zr}_2(\text{PO}_4)_3 (\text{s}) + \frac{1}{2}\text{CuO} (\text{s}) \leftrightarrow \text{CuZr}_2(\text{PO}_4)_3 (\text{s}) + \frac{1}{4}\text{O}_2 (\text{g})$  was studied by thermogravimetry in an atmosphere of  $P_{\text{O}_2} = 0.22$  atm and was found to occur at  $475 \pm 10^\circ\text{C}$ . Thus,  $\text{CuZr}_2(\text{PO}_4)_3$  is a thermodynamically stable phase in air above  $\sim 475^\circ\text{C}$ , which places a lower temperature limit on its use as an electrolyte in air. The results of X-ray powder diffractometry on materials with various copper contents that had been annealed in argon at  $750^\circ\text{C}$  indicate that there is no evidence for a significant solid solution between  $\text{CuZr}_2(\text{PO}_4)_3$  and  $\text{Cu}_{0.5}\text{Zr}_2(\text{PO}_4)_3$  nor, a reductive decomposition of  $\text{Cu}_{0.5}\text{Zr}_2(\text{PO}_4)_3$ . The coexistence of  $\text{CuZr}_2(\text{PO}_4)_3$  and  $\text{Cu}_{0.5}\text{Zr}_2(\text{PO}_4)_3$  as discrete phases is also supported by evidence from electron spin resonance spectroscopy on these materials, which indicate the presence of copper(II) ions in  $\text{CuZr}_2(\text{PO}_4)_3$  at a dopant and dispersed level of concentration. The results from energy dispersive X-ray analysis, as well as, the novel use of the fluorescent behaviour of  $\text{CuZr}_2(\text{PO}_4)_3$  in ultra-violet light as an analytical tool, support the above conclusions.

© 2006 Springer Science + Business Media, Inc.

## 1. Introduction

Since the discovery of fast sodium ion transport in  $\text{Na}_{1+x}\text{Zr}_2\text{Si}_x\text{P}_{3-x}\text{O}_{12}$  ( $0 \leq x \leq 3$ ) by Hong in 1976 [1], many other Nasicon related phases have been discovered. One such phase is the copper phosphate analogue material  $\text{CuZr}_2(\text{PO}_4)_3$  (with the acronym ‘Cusicon’) as first reported by Yao and Fray in 1983 and shown to be a copper(I) ionic conductor [2].

The Nasicon crystal structure is shown in Fig. 1. The structure consists of a three-dimensional substructure comprising  $\text{ZrO}_6$  octahedra corner sharing six  $\text{SiO}_4$  (or  $\text{PO}_4$ ) tetrahedra. The sodium ions are accommodated within two large, but distinct, crystallographic sites within this substructure, designated M(1) and M(2). What is particularly interesting is that these two sites are interconnected with one another in a three-dimensional manner, such that each M(1) site is connected to six M(2) sites, and each M(2) site is connected to two M(1) sites, as shown in Fig. 2. This connection leads to the infinite

sequence: M(1)-M(2)-M(1)-M(2)-... etc. in three dimensional space; which forms the conduction pathway for the mobile sodium ions.

The crystal structure for  $\text{CuZr}_2(\text{PO}_4)_3$  is shown in Fig. 3, which is based upon the neutron powder diffraction data given by I. Bussereau *et al.* [3]. This figure shows how the copper(I) ions are distributed between six off-centred equivalent positions in the M(1) site, which gives rise to the ‘daisy-wheel’ like features in the diagram; the M(2) site being vacant. In this M(1) site there are two short Cu–O bonds of 2.05 Å and four longer Cu–O bonds of 2.70 Å. This is a result of the unusual copper(I) coordination which appears to be a compromise between the usual linear (dumb-bell) coordination and the antiprismatic geometry of the M(1) site created by the ‘ $\text{Zr}_2(\text{PO}_4)_3$ ’ substructure [3]. It is interesting to note, that as a consequence of the huge size of the M(1) site, it is possible to have two copper(I) ions within the same M(1) site. From a study using, extended X-ray absorption fine

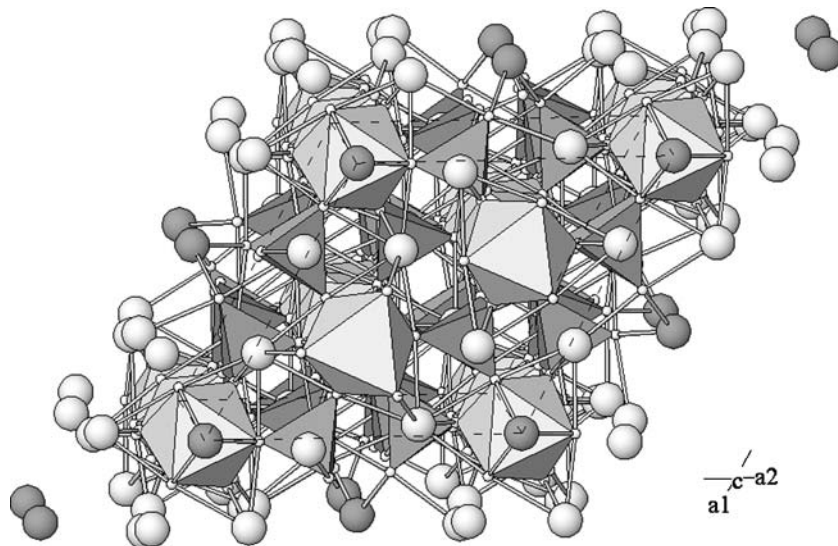


Figure 1 Crystal structure of Nasicon ( $\text{Na}_4\text{Zr}_2(\text{SiO}_4)_3$ ) based on the data given in ICDS file number #38055. The hexagonal symmetry is evident. The M(1) sites are shown as grey spheres, and the M(2) sites are shown as white spheres.

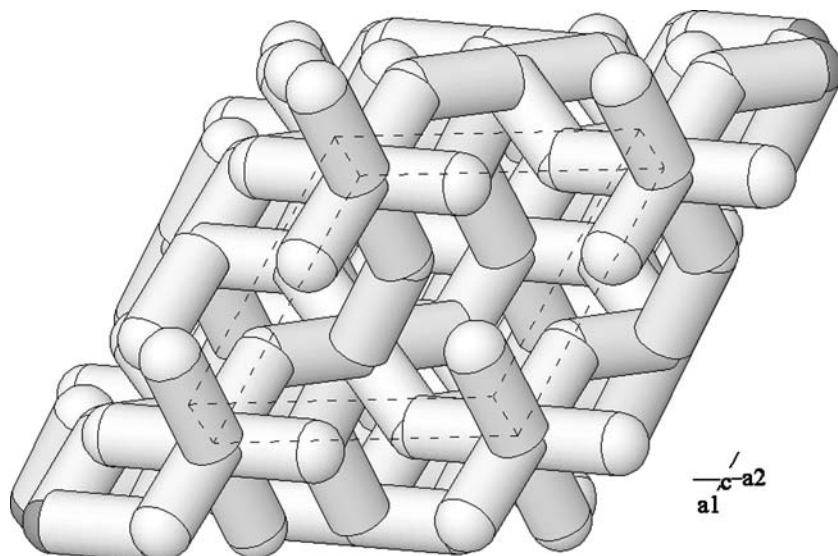


Figure 2 Diagram showing the conduction pathways between the M(1) and M(2) sites in the Nasicon structure. The M(1) sites are shown as grey spheres (or are hidden from view), and the M(2) sites are shown as white spheres.

structure (EXAFS), E. Fargin *et al.* [4, 5] showed that  $\sim 20\%$  of the M(1) sites are occupied by  $\text{Cu}^{\text{I}}\text{-Cu}^{\text{I}}$  pairs,  $\sim 60\%$  are singularly occupied by copper(I) ions and the remaining  $\sim 20\%$  are empty. Indeed, the presence of a  $\text{Cu}^{\text{I}}\text{-Cu}^{\text{I}}$  pair with an internal Cu-Cu distance of  $2.40 \text{ \AA}$  is considered to be the source of the luminescent behaviour of  $\text{CuZr}_2(\text{PO}_4)_3$ , which is strongly fluorescent under UV-light at room temperature, where it emits a green fluorescent band at  $540 \text{ nm}$  [6, 7].

The copper(II) analogue material  $\text{Cu}_{0.5}\text{Zr}_2(\text{PO}_4)_3$  has been prepared by several methods including; chemical oxidation of the copper(I) precursor material with the subsequent removal of exsolved copper(II)oxide with dilute aqueous acids [8] and, by sol-gel (alkoxide) methods [9, 10]. The nature of the material, such as, the refined aspects of its crystal structure (as interpreted from powder XRD) and colour, appear to be very dependent on the prepara-

tion method. An ESR study of  $\text{Cu}_{0.5}\text{Zr}_2(\text{PO}_4)_3$  by Taoufik *et al.* [11] suggests that the copper(II) ions are distributed among both the M(1) and M(2) sites, but with a preference for the M(1) site. However, to the best of our knowledge, single crystal XRD or, neutron powder diffraction data for  $\text{Cu}_{0.5}\text{Zr}_2(\text{PO}_4)_3$ , are not available in the literature and, therefore, the copper site occupation factors relating to the M(1) and M(2) sites within the structure are not known with certainty.

In a more general context relating to mixed-valence systems, the possibility for copper to exist in more than one oxidation state within the same structural framework is well known; a relevant example being the mixed-valence copper orthophosphate  $\text{Cu}^{\text{I}}\text{Cu}^{\text{II}}\text{Mg}_3(\text{PO}_4)_3$  [12]. The question which then beckons, is whether this is possible within the Cusicon-type framework corresponding to  $\text{Cu}^{\text{I/II}}_{1-x}\text{Zr}_2(\text{PO}_4)_3$  ( $0 \leq x \leq 0.5$ ). Indeed, a controversial

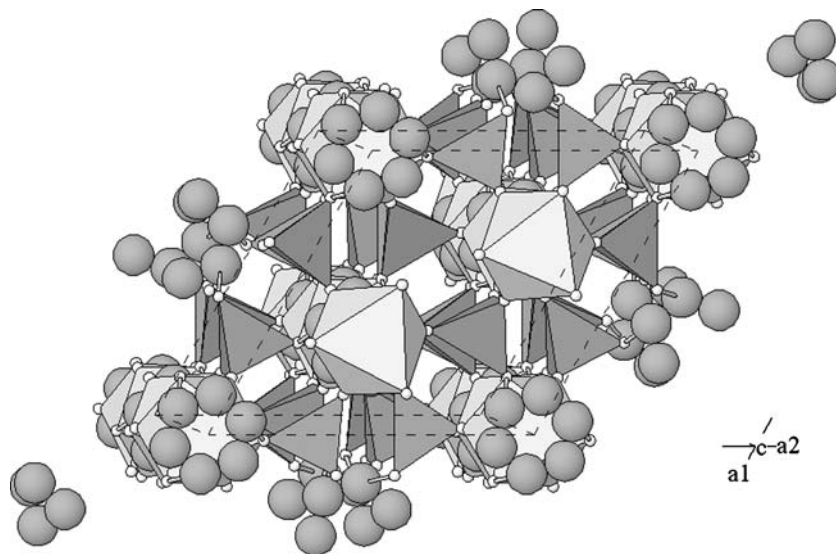


Figure 3 Crystal structure of  $\text{CuZr}_2(\text{PO}_4)_3$  based on the data given in ICDS file number #71881. The distorted nature of the copper sites appear like “daisy-wheels” running parallel to the  $a(1)$ - $a(2)$  basal plane.

issue for many years has been the question concerning the possible existence of a solid solution (either partial or continuous) between  $\text{CuZr}_2(\text{PO}_4)_3$  and  $\text{Cu}_{0.5}\text{Zr}_2(\text{PO}_4)_3$ . For instance, Schaffer, in his doctoral thesis [13], makes reference to such a solid solution whilst, Davidson and Fray [14] refer to a sintered Cusicon material with the empirical formula ‘ $\text{Cu}_{0.8}\text{Zr}_2(\text{PO}_4)_3$ ’. Furthermore, Cusicon has been prepared as a colourless, as well as, a green coloured material of various shades, by different workers [2, 14–17]. Therefore, it would be interesting to see if this variation in colour is due to the presence of copper(II) ions at a defect level of concentration or, at a higher concentration more appropriately described by a solid solution of some defined extent.

In a technological context, this bivalent feature can sometimes be a nuisance. For example, in situations in which the presence of copper(I) ions is essential to the intended function of the device, such as, the copper(I) solid electrolyte inside a chemical sensor, battery or other electrochemical membrane. Here, any oxidation to copper(II) ions should be avoided since this may adversely alter the electrical properties of the material. The formation of copper(II) ions can take place essentially, in one of two ways. By chemical or electrochemical oxidation ( $\text{Cu}^+ \rightarrow \text{Cu}^{2+} + e^-$ ) and, by disproportionation ( $2\text{Cu}^+ \rightarrow \text{Cu}^{2+} + \text{Cu}$ ). Either way, the changes in Gibbs free energy for the reactions involved are either explicit or implicit functions of copper activity. Therefore, an understanding of the interrelationships between copper activity, stoichiometry, valence, and the existence of any solid solutions within this class of materials, is crucial to any meaningful exploitation of their electrical properties. In connection with these phase relationships, is the issue concerning the thermodynamic stability of  $\text{CuZr}_2(\text{PO}_4)_3$  in terms of temperature and oxygen fugacity.

The results of various experiments including; powder X-ray diffractometry (XRD), thermogravimetry, electron spin resonance (ESR) spectroscopy, energy dispersive X-ray analysis (EDXA) and observations made under ultra-violet light, aimed at resolving these issues, are presented here.

## 2. Experimental

### 2.1. Synthesis of $\text{CuZr}_2(\text{PO}_4)_3$

Copper(II) oxide (99%, Aldrich), ammonium dihydrogen phosphate (99%, Merck) and zirconium(IV) oxide (99.9%, Aldrich) were weighed in appropriate amounts and mixed in a micromill overnight with acetone as a dispersion agent. The resulting mixture, after the evaporation of the acetone in air, was placed in an alumina crucible and slowly heated in a box furnace (Vecstar Furnaces VF 1 SP) to  $400^\circ\text{C}$  and held at that temperature overnight in order to decompose the  $\text{NH}_4\text{H}_2\text{PO}_4$  and initiate the first stage of the reaction [15]. The product material was slowly cooled to room temperature, then ground with an agate pestle and mortar. The powdered material was placed in a boat-shaped alumina crucible and introduced into a tube furnace (Lenton Furnaces LTF 16/50/180) attached with a recrystallized alumina worktube. The material was heated to  $1200^\circ\text{C}$  for 16 h, in a flowing argon (99.99%, Hede Nielsen A/S) atmosphere, with heating and cooling rates both set at  $5^\circ\text{C}/\text{min}$ . The product was analysed by powder XRD.

### 2.2. Synthesis of $\text{Cu}_{0.5}\text{Zr}_2(\text{PO}_4)_3$

$\text{Cu}_{0.5}\text{Zr}_2(\text{PO}_4)_3$  was prepared by an indirect method. The precursor material comprised a finely ground powder of  $\text{CuZr}_2(\text{PO}_4)_3$  as prepared above. This material was placed inside an alumina crucible and oxidized in air, inside a

box furnace at 400°C, then cooled to room temperature. The product material was ground with an agate pestle and mortar. The above oxidation process was repeated to ensure complete oxidation of the material. Finally, the powdered product was washed with warm dilute nitric acid to remove the copper(II) oxide, followed by a wash with distilled water, then subsequently dried in air. The product was analysed by powder XRD using a Siemens D5000 diffractometer using Cu-K $\alpha_1$  radiation.

### 2.3. Magnetic measurements

X-band (9.3404 GHz) ESR spectra were obtained using a Bruker Biospin EMX-system spectrometer employing a 100 kHz field modulation. Measurements were carried out at 77 K.

### 2.4. Thermogravimetry

Thermogravimetric measurements were made using a modified instrument (TG 92-12 Setaram). The instrument was operated with a controlled atmosphere, which was supplied by mixing oxygen (99.5%, Hede Nielsen A/S) with argon (99.99%, Hede Nielsen A/S) in different ratios. The contents of the atmosphere were determined by 'on-line' mass spectroscopy. A powdered sample of CuZr $_2$ (PO $_4$ ) $_3$  was placed in a miniature alumina crucible and heated with a rate of 1°C/min from room temperature to 1000°C in an atmosphere of  $P_{O_2} = 0.22$  atm, and maintained for one hour, then followed by cooling to room temperature at the same rate.

### 2.5. Investigations concerning the possible existence of a solid solution

Powders of colourless CuZr $_2$ (PO $_4$ ) $_3$  and pale-blue Cu $_{0.5}$ Zr $_2$ (PO $_4$ ) $_3$  were weighed together with formula-unit ratios of 3:1 and 1:1 respectively. In each case, the thoroughly mixed powder was placed inside a silicon rubber mould (manufactured in-house) which in turn was held and tied inside a condom, before being pressed at 15 kbar for 30 minutes using an oil-press (20 kbars Pressure Reaction System, supplied by PSIKA Pressure Systems Ltd.) in order to form a densely compacted pellet. The pellet was then heated to 750°C for 16 hours in 99.99% argon. These conditions should be sufficient, in terms of temperature, time, and pellet density to enable any envisaged formation of a solid solution to take place, by the inter-diffusion of copper ions within this two phase mixture. After heat treatment, the pellet was quenched to room temperature and then ground using an agate pestle and mortar. The powdered material was analysed by ESR and powder XRD.

A third pellet was prepared by a method for making 'double-layered' pressed powdered pellets. A layer of Cu $_{0.5}$ Zr $_2$ (PO $_4$ ) $_3$  powder was placed in the bottom half of the silicon rubber mould, and followed by a layer of CuZr $_2$ (PO $_4$ ) $_3$  powder in the top half of the mould. This

was then pressed at 15 kbar for 30 minutes into a single pellet using the oil press as described above. The pellet was first heated at 750°C in flowing argon (99.99%) for 16 hours and then cooled to room temperature. Observations were made on the pellet before re-annealing under identical conditions for a further 160 hours. After this time, the pellet was dissected longitudinally, such that the cross-section was observed under ultra-violet light and also analysed by electron microscopy and dispersive X-ray analysis (EDXA) using a Jeol JSM-35CF scanning microscope.

## 3. Results and discussion

### 3.1. Powder XRD of prepared materials

In this work, CuZr $_2$ (PO $_4$ ) $_3$  was obtained as a colourless powder whilst, Cu $_{0.5}$ Zr $_2$ (PO $_4$ ) $_3$  was obtained as a pale-blue powder. The powder XRD patterns for the materials, CuZr $_2$ (PO $_4$ ) $_3$  and Cu $_{0.5}$ Zr $_2$ (PO $_4$ ) $_3$  as prepared here, are shown in Figs 4 and 5 respectively. Their  $d$ -values and relative intensities for these phases correspond closely to those reported in the ICDD card numbers 81-0526 and 42-1057 respectively. Interestingly, one additional peak ( $2\theta = 25.75^\circ$ , relative intensity = 17) appears in the powder pattern for the CuZr $_2$ (PO $_4$ ) $_3$  material prepared in this work, with a  $d$ -value = 3.457 Å; but it has not been possible to either index this peak or, account for its presence.

### 3.2. Thermogravimetric analysis of CuZr $_2$ (PO $_4$ ) $_3$

Fig. 6 shows the thermogravimetric profile for CuZr $_2$ (PO $_4$ ) $_3$  in an oxygen partial pressure of 0.22 atm. This shows a gradual and continuous gain in mass from room temperature upwards, which is interpreted in terms of oxidation of the material until  $475 \pm 10^\circ\text{C}$ . Above this temperature the material gradually loses mass, which is interpreted in terms of a loss of oxygen from the system and is associated with the reduction of the material. Later in the heating-cycle, when the sample is eventually cooled below  $475 \pm 10^\circ\text{C}$ , there is a regain in mass corresponding to the addition of oxygen to the system. This mass-temperature profile is therefore interpreted in terms of a reversible uptake and release of oxygen from the material. Similar observations have been reported for CuHf $_2$ (PO $_4$ ) $_3$  [18] and CuSn $_2$ (PO $_4$ ) $_3$  [19], whereby the redox-transition equilibrium temperatures are approximately 500°C and 480°C respectively. Given the close structural similarities between these three compounds it is quite reasonable to expect a similarity in their redox-transition equilibrium temperatures.

This analysis confirms that CuZr $_2$ (PO $_4$ ) $_3$  is a metastable phase at room-temperature and under atmospheric conditions ( $T = 298$  K and  $P_{O_2} = 0.22$  atm). Therefore, as the temperature increases, CuZr $_2$ (PO $_4$ ) $_3$  begins to oxidize

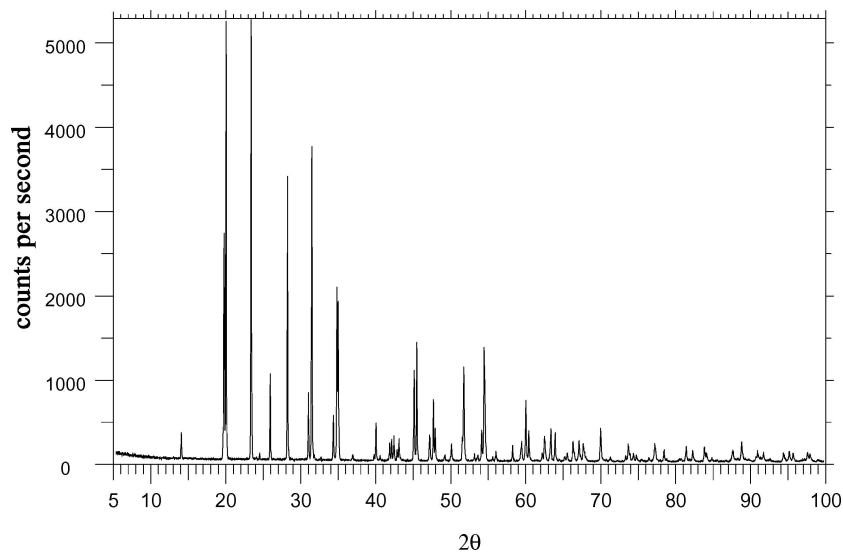


Figure 4 Powder X-ray diffraction pattern for  $\text{CuZr}_2(\text{PO}_4)_3$  using  $\text{Cu-K}\alpha_1$  radiation.

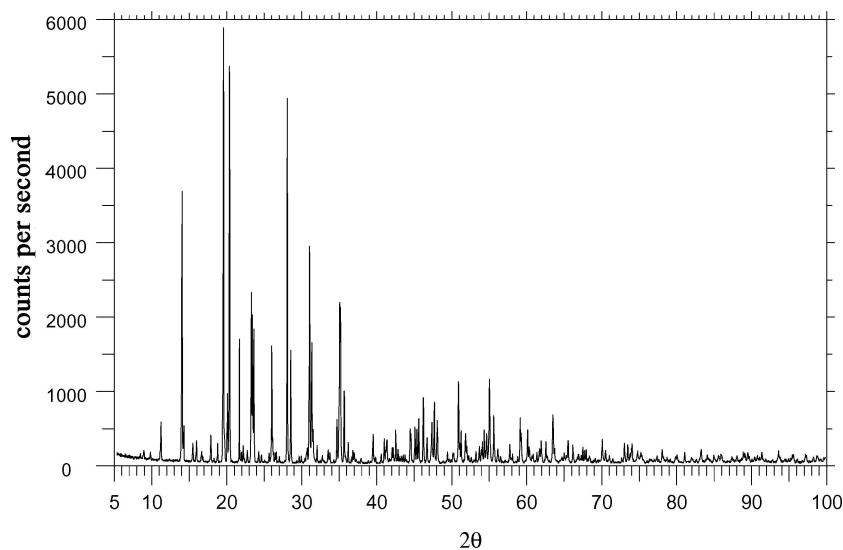


Figure 5. Powder X-ray diffraction pattern for  $\text{Cu}_{0.5}\text{Zr}_2(\text{PO}_4)_3$  using  $\text{Cu-K}\alpha_1$  radiation.

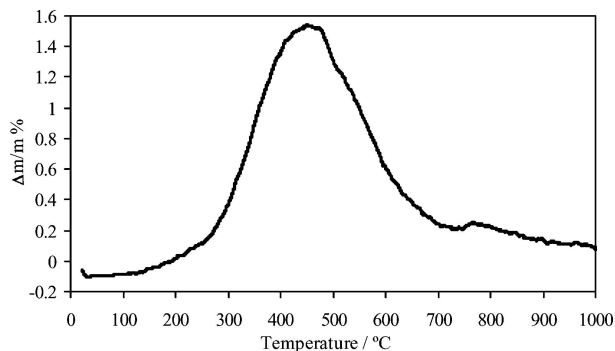
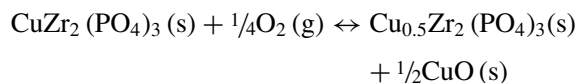


Figure 6 Thermogravimetric profile for  $\text{CuZr}_2(\text{PO}_4)_3$  under an oxygen partial pressure of 0.22 atm.

to  $\text{Cu}_{0.5}\text{Zr}_2(\text{PO}_4)_3$  and  $\text{CuO}$ . However, once the temperature rises above the redox-transition temperature ( $T_{\text{redox}}$ ), the material (an intimate mixture of  $\text{Cu}_{0.5}\text{Zr}_2(\text{PO}_4)_3$  and

$\text{CuO}$ ) begins to revert back to  $\text{CuZr}_2(\text{PO}_4)_3$ , with a corresponding loss of oxygen from the system. It is therefore concluded that  $\text{CuZr}_2(\text{PO}_4)_3$  is a thermodynamically stable phase at a temperature,  $T \geq 475 \pm 10^\circ\text{C}$  (at  $P_{\text{O}_2} = 0.22$  atm). This implies that  $\text{CuZr}_2(\text{PO}_4)_3$  should retain its predominant copper(I) ionic conducting properties in air, at high temperature ( $\geq 475 \pm 10^\circ\text{C}$ ); as is the case under inert atmospheric conditions, such as argon [15, 17].

Schaffer *et al.* [16] performed a series of electrochemical measurements on a solid state electrochemical cell using a ceramic disc of  $\text{CuZr}_2(\text{PO}_4)_3$  as one of the ‘electrodes’. From their work they derived the following expression for the temperature dependence (in Kelvin) on the equilibrium partial pressure of oxygen, for the equilibrium reaction:



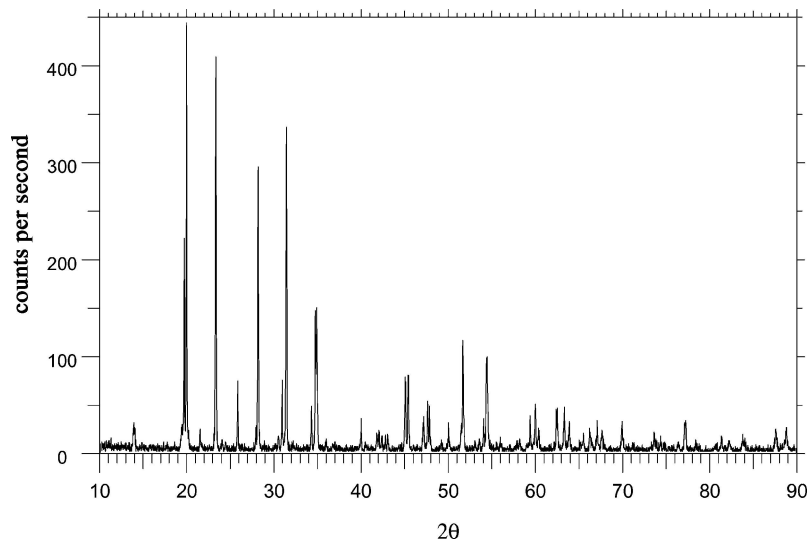


Figure 7 Powder X-ray diffraction pattern for the  $\text{CuZr}_2(\text{PO}_4)_3$  sample quenched from  $700^\circ\text{C}$  in air, using  $\text{Cu-K}\alpha_1$  radiation.

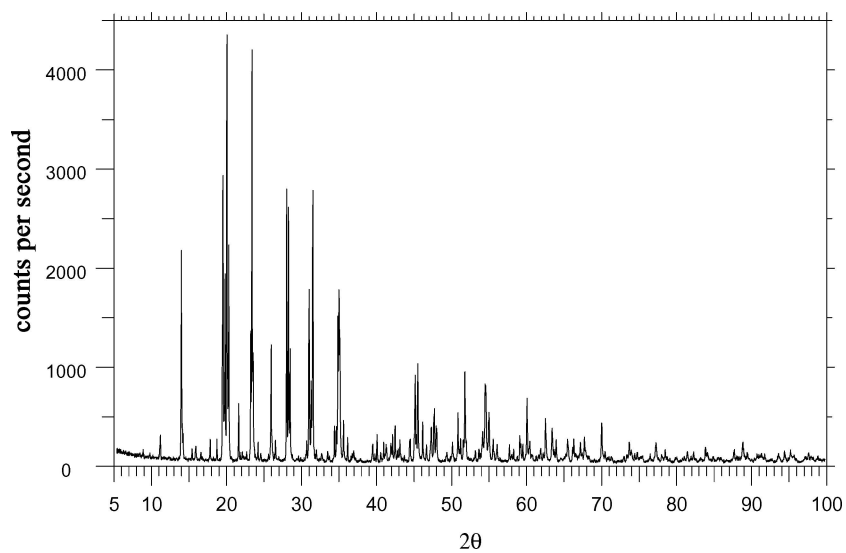


Figure 8 Powder X-ray diffraction patterns for  $\text{CuZr}_2(\text{PO}_4)_3/\text{Cu}_{0.5}\text{Zr}_2(\text{PO}_4)_3$  in the molar ratio 3:1 after the heat treatment described in Section 2.5, using  $\text{Cu-K}\alpha_1$  radiation.

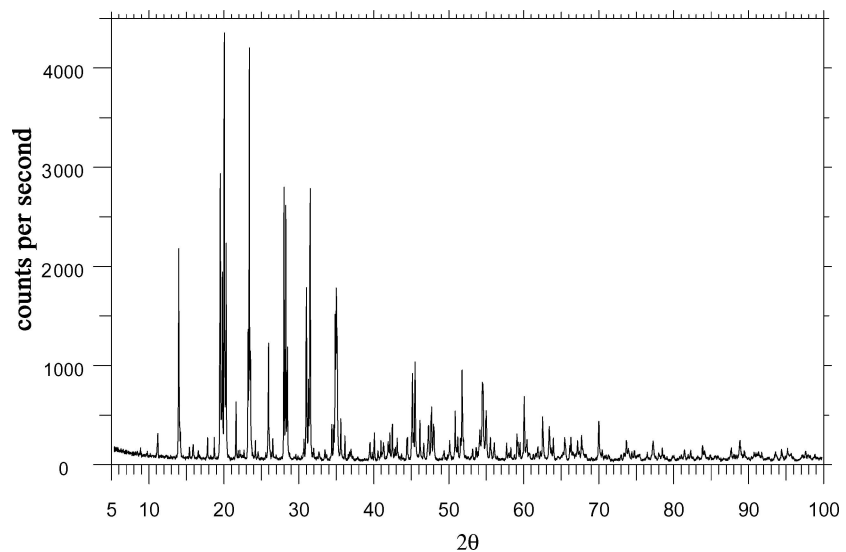


Figure 9 Powder X-ray diffraction patterns for  $\text{CuZr}_2(\text{PO}_4)_3/\text{Cu}_{0.5}\text{Zr}_2(\text{PO}_4)_3$  in the molar ratio 1:1 after the heat treatment described in Section 2.5, using  $\text{Cu-K}\alpha_1$  radiation.

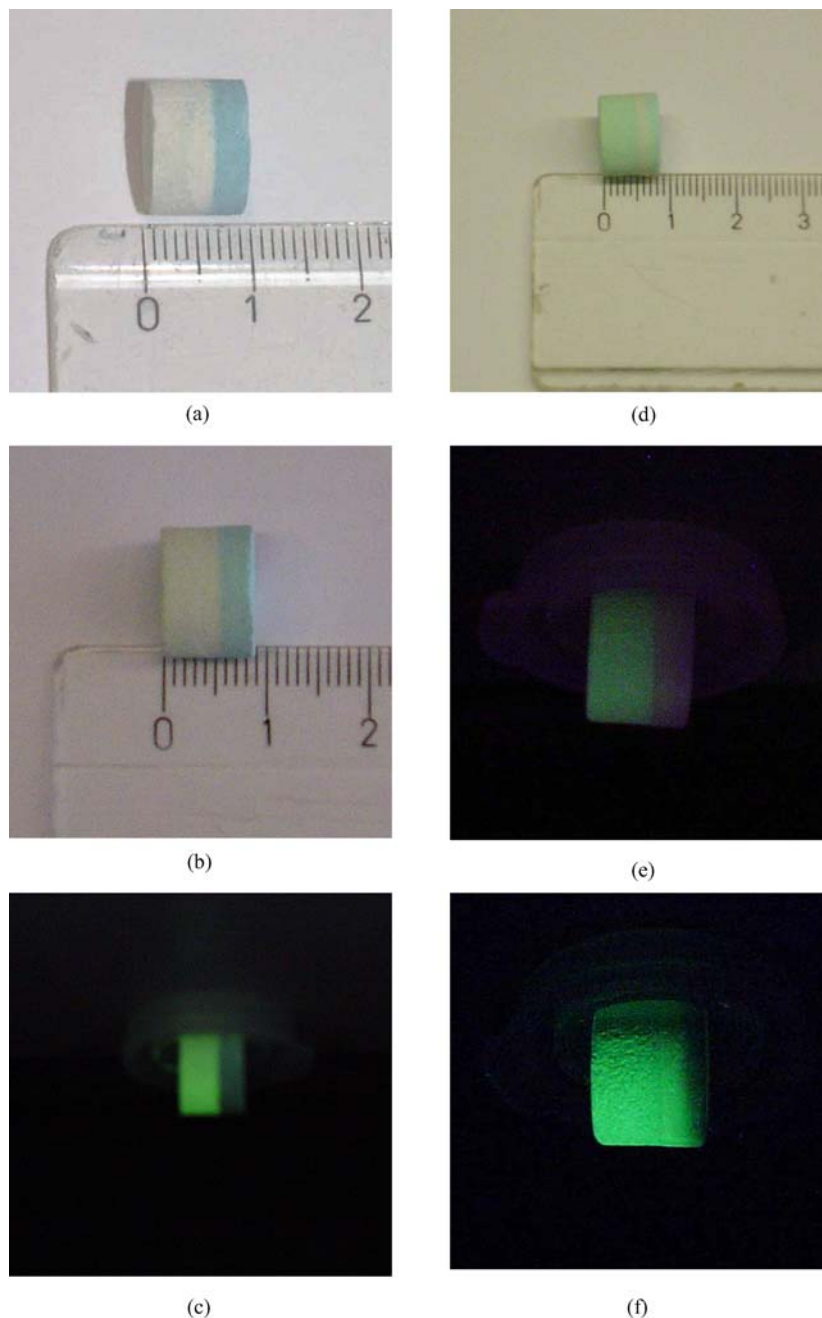


Figure 10 Photographs of the layered pellets taken under various types of illumination before and after annealing. See text for detailed descriptions.

$$\log_{10}(P_{O_2}/\text{atm}) = 18.341 - 22729T^{-1}$$

where  $T$  is absolute temperature in Kelvin and,  $P_{O_2}$  is presumed to be in units of atmosphere. Applying this expression to the above system under an atmosphere of air ( $P_{O_2} = 0.21$  atm) yields an equilibrium temperature of 1195 K (922°C). This value is significantly higher than the one obtained in this present work, viz. 475°C (which is based on the results of thermogravimetry).

To investigate this system further, a powdered sample of  $\text{CuZr}_2(\text{PO}_4)_3$  was annealed at 700°C in air ( $P_{O_2} = 0.21$  atm) for 2 hours, then poured immediately onto a large block of aluminium in order to quench the material

to room temperature. The product material was essentially a colourless powder with a pale-green tinge in places. The powder XRD pattern is shown in Fig. 7. Besides an additional peak ( $2\theta = 25.75^\circ$ ) which has previously been commented on in Section 3.1, this pattern indicates that  $\text{CuZr}_2(\text{PO}_4)_3$  was the only phase detectable by this technique. This shows that the material exists essentially in its reduced (cuprous) form,  $\text{CuZr}_2(\text{PO}_4)_3$  at 700°C in air. From the electrochemical studies of Schaffer *et al.* [16], one is left to infer, from their interpretation of electrochemical data, that the material should exist in its oxidized form under these conditions; in other words, as a two phase mixture of  $\text{Cu}_{0.5}\text{Zr}_2(\text{PO}_4)_3$  and  $\text{CuO}$ . This is in contradiction to the observations made here in this

present work. Perhaps the Cusicon ‘electrode’ as used by Schaffer *et al.* [16] is not at a state of equilibrium or functioning in a manner, as they have presumed in their work.

### 3.3. Investigation of a solid solution between $\text{CuZr}_2(\text{PO}_4)_3$ and $\text{Cu}_{0.5}\text{Zr}_2(\text{PO}_4)_3$

Due to the high mobility of the copper(I) ions within the Cusicon frame work structure [2, 15, 17], if, a solid solution did exist between  $\text{CuZr}_2(\text{PO}_4)_3$  and  $\text{Cu}_{0.5}\text{Zr}_2(\text{PO}_4)_3$ , one would expect it to form during the annealing of a finely compacted mixture of  $\text{CuZr}_2(\text{PO}_4)_3$  and  $\text{Cu}_{0.5}\text{Zr}_2(\text{PO}_4)_3$  powders at high temperature under an inert atmosphere. Figs 8 and 9 show the powder XRD patterns for the samples comprising initial mixtures of  $\text{CuZr}_2(\text{PO}_4)_3$  and  $\text{Cu}_{0.5}\text{Zr}_2(\text{PO}_4)_3$  in the molar ratios of 3:1 and 1:1 respectively, recorded *after* the heat treatment as described in Section 2.5. Both of these powder patterns reveal a mechanical mixture of just two discrete phases;  $\text{CuZr}_2(\text{PO}_4)_3$  and  $\text{Cu}_{0.5}\text{Zr}_2(\text{PO}_4)_3$  after the heat treatment performed here. It is therefore concluded that a solid solution does not exist at 750°C. Neither is there evidence of any reductive decomposition of  $\text{Cu}_{0.5}\text{Zr}_2(\text{PO}_4)_3$  under these conditions.

Figs 10a and b show respectively, pictures taken under normal white light of the ‘double-layered’ pellet, *before* and *after* the 16 hours of annealing as described in Section 2.5; revealing colourless  $\text{CuZr}_2(\text{PO}_4)_3$  on the left and pale-blue  $\text{Cu}_{0.5}\text{Zr}_2(\text{PO}_4)_3$  on the right. Fig. 10c shows the same as Fig. 10b, but is taken under ultra-violet light ( $\lambda = 366 \text{ nm}$ ); revealing the green-fluorescence from  $\text{CuZr}_2(\text{PO}_4)_3$  on the left and non-fluorescence from  $\text{Cu}_{0.5}\text{Zr}_2(\text{PO}_4)_3$  on the right. The presence of two clearly segregated regions suggests there is no significant inter-diffusion of copper between these two layers after 16 hours of annealing at 750°C.

Fig. 10d shows a picture taken under normal white light after annealing for a further 160 hours at 750°C in argon; revealing pale-green material on the left and a pale-blue material on the far-right with a colourless material in the interfacial region. Figs 10e and f show a longitudinal cross-section of the same pellet (as in Fig. 10d) but taken under ultra-violet light;  $\lambda = 254 \text{ nm}$  and 366 nm respectively. These observations suggest that some inter-diffusion has occurred between  $\text{CuZr}_2(\text{PO}_4)_3$  and  $\text{Cu}_{0.5}\text{Zr}_2(\text{PO}_4)_3$  after prolonged annealing, although the original segregation is still clearly visible in Fig. 10e. Table I shows the results from the energy dispersive X-ray analysis (EDXA) performed on this cross-section of the pellet. These results indicate a difference in copper concentration across the pellet longitudinally, corresponding to a high copper content in both the colourless and pale-green regions and, a significantly lower copper concentration in the pale-blue region, as described above. After such prolonged annealing, it is evident that the material is still very inhomogeneous. In terms of microstructure, the inter-diffusion region of the pellet is more appropriately described as a fine-grained mechanical mixture of two

TABLE I Energy dispersive X-ray analysis (EDXA) of the cross-section of the double-layered pellet. The values are quoted as mean values from the total Cu + Zr analysis and are presented as atomic percentages

	Cu (at.%)	Zr (at.%)	Atomic ratio Cu:Zr
Pale-blue area	22.77	77.23	~1:4
Colourless area	30.25	69.75	~1:2
Pale-green area	32.54	67.46	~1:2

distinct phases ( $\text{CuZr}_2(\text{PO}_4)_3$  and  $\text{Cu}_{0.5}\text{Zr}_2(\text{PO}_4)_3$ ) rather than a solid solution.

Taufik *et al.* [11] have performed an ESR study on  $\text{Cu}_{0.5}\text{Zr}_2(\text{PO}_4)_3$ . Their work revealed very broad spectra, and was interpreted in terms of copper(II) ions being distributed between the M(1) and M(2) sites in the approximate ratio 2:1 respectively. The results of a series of ESR measurements performed on the various compositional mixtures investigated in this present work are shown in Fig. 11. The absolute concentrations are difficult to quantify by this technique, but nonetheless, the copper(II) signal in  $\text{CuZr}_2(\text{PO}_4)_3$  is particularly weak. This indicates the presence of copper(II) ions as a dopant and at a dispersed level of concentration in the colourless to pale-green material. The  $\text{Cu}_{0.5}\text{Zr}_2(\text{PO}_4)_3$

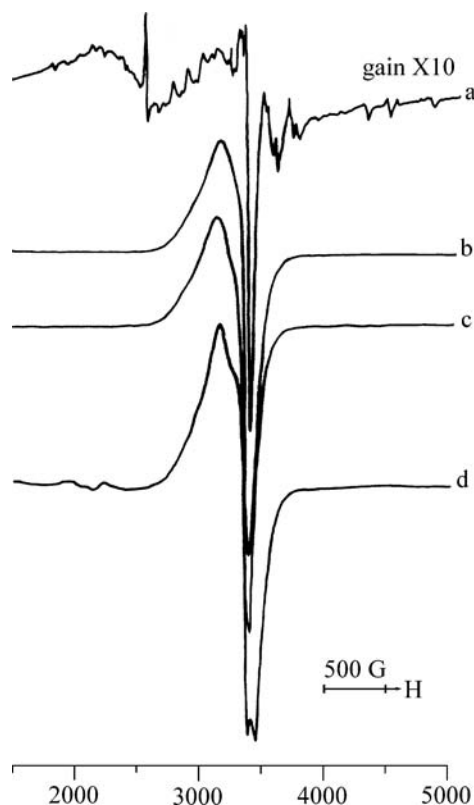


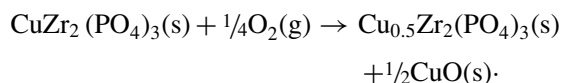
Figure 11 First derivative X-band ESR spectra of the following materials recorded at 77 K and attributed to copper(II) ions. (a) Colourless to pale-green  $\text{CuZr}_2(\text{PO}_4)_3$  (gain X10). (b)  $\text{CuZr}_2(\text{PO}_4)_3/\text{Cu}_{0.5}\text{Zr}_2(\text{PO}_4)_3$  in the molar ratio 3:1 recorded *after* the heat treatment described in Section 2.5. (c)  $\text{CuZr}_2(\text{PO}_4)_3/\text{Cu}_{0.5}\text{Zr}_2(\text{PO}_4)_3$  in the molar ratio 1:1 recorded *after* the heat treatment described in Section 2.5. (d) Pale-blue  $\text{Cu}_{0.5}\text{Zr}_2(\text{PO}_4)_3$ .



material gave a very broad peak similar to that reported by Taoufik *et al.* [11], whilst the  $\text{CuZr}_2(\text{PO}_4)_3$  material gave a very sharp peak. Intermediate compositions gave very broad peaks. These aspects concerning the peak width are used here to show that there is no evidence of a solid solution in these intermediate compositions. If any significant solid solution did occur, then progressive line broadening would be expected across the compositional series.

#### 4. Conclusions

$\text{CuZr}_2(\text{PO}_4)_3$  is a metastable phase under ambient temperature and atmospheric conditions ( $T = 25^\circ\text{C}$  and  $P_{\text{O}_2} = 0.21$  atm). The pertinent reaction being:



The results from thermogravimetry performed on this material under an atmosphere of  $P_{\text{O}_2} = 0.22$  atm. give a value for the corresponding equilibrium temperature for the above reaction as  $475 \pm 10^\circ\text{C}$ .  $\text{CuZr}_2(\text{PO}_4)_3$  should therefore function as a copper(I) ionic conductor in air above  $\sim 475^\circ\text{C}$ , even after a long exposure time to air; but not below this temperature. This is different to the situation when  $\text{CuZr}_2(\text{PO}_4)_3$  is used under an inert atmosphere; in which a lower temperature restriction on its use is then, normally, dictated by the magnitude of its ionic conductivity.

This present work has indicated that there is no evidence for a continuous solid solution between  $\text{CuZr}_2(\text{PO}_4)_3$  and  $\text{Cu}_{0.5}\text{Zr}_2(\text{PO}_4)_3$ ; and especially not within the compositional range  $\text{Cu}_{1-x}\text{Zr}_2(\text{PO}_4)_3$  ( $0.125 \leq x \leq 0.25$ ) at  $750^\circ\text{C}$ . However, the results suggest that the pale-green to colourless material corresponds to a solid solution of a *very limited* extent, described by,  $\text{Cu}^{\text{I/II}}_{1-x}\text{Zr}_2(\text{PO}_4)_3$  ( $0 \leq x \ll 0.125$ ), which is more akin to the presence of copper(II) ions at a dopant and dispersed level of concentration. The presence of these copper defects is not expected to affect the ionic conducting properties of this material by any great extent.

The absence of a solid solution may be due to the peculiar co-ordination environments of the copper(I) and copper(II) ions in these materials. Although the substructural frameworks of  $\text{CuZr}_2(\text{PO}_4)_3$  and  $\text{Cu}_{0.5}\text{Zr}_2(\text{PO}_4)_3$  are closely related, the co-ordination of copper(I) and copper(II) ions in the M(1) position are very different, which leads to local distortions. This might explain why copper(I) and copper(II) ions cannot be accommodated simultaneously within a single Nasicon-type phase, except when present at a defect level of concentration. It would be interesting to compare these aspects with related systems, such as,  $\text{CuTi}_2(\text{PO}_4)_3 - \text{Cu}_{0.5}\text{Ti}_2(\text{PO}_4)_3$ ,  $\text{CuHf}_2(\text{PO}_4)_3 - \text{Cu}_{0.5}\text{Hf}_2(\text{PO}_4)_3$  and  $\text{CuSn}_2(\text{PO}_4)_3 - \text{Cu}_{0.5}\text{Sn}_2(\text{PO}_4)_3$ , as

well as, to obtain single crystal X-ray diffraction or, neutron diffraction data for the cupric phase,  $\text{Cu}_{0.5}\text{Zr}_2(\text{PO}_4)_3$ .

The fluorescent behaviour of  $\text{CuZr}_2(\text{PO}_4)_3$  under ultra-violet light has proved to be useful as a simple analytical tool in this work.

#### Acknowledgment

The authors are grateful to Miss T. Knudsen for assistance with the electron microscopy and energy dispersive X-ray analysis, and to Prof. H. Toftlund-Nielsen for help with interpreting the electron spin resonance spectroscopic measurements. One of the authors (TEW) would like to thank Prof. D.J. Fray for the many fruitful discussions concerning 'Cusicon' over the years. The crystal structure drawings were produced with ATOMS, by Shape Software.

#### References

1. H. Y.-P. HONG, *Mat. Res. Bull.* **11** (1976) 173.
2. P. C. YAO and D. J. FRAY, *Solid State Ionics* **8** (1983) 35.
3. I. BUSSEREAU, M. S. BELKHIRIA, P. GRAVEREAU, A. BOIREAU, J. L. SOUBEYROUX, R. OLAZCUAGAL and G. LE FLEM, *Acta Cryst.* **C48** (1992) 1741.
4. E. FARGIN, I. BUSSEREAU, G. LE FLEM, R. OLAZCUAGAL, C. CARTIER and H. DEXPERT, *Eur. J. Solid State Inorg. Chem.* **29** (1992) 975.
5. E. FARGIN, I. BUSSEREAU, R. OLAZCUAGAL and G. LE FLEM, *J. Solid State Chem.* **112** (1994) 176.
6. B. MAIHOLD and H. WULFF, *Wiss. Z. Ernst-Moritz-Arndt-Unt. Greifswald, Math.-nat.wiss. Reihe* **36** (1987) 27.
7. G. LE POLLES, C. PARENT, R. OLAZCUAGAL, G. LE FLEM and P. HAGENMULLER, *C. R. Acad. Sci. Paris* **306** Série II (1988) 765.
8. A. EL JAZOULI, M. ALAMI, R. BROCHU, J. M. DANCE, G. LE FLEM and P. HAGENMULLER, *J. Solid State Chem.* **71** (1987) 444.
9. I. BUSSEREAU, R. OLAZCUAGAL, G. LE FLEM and P. HAGENMULLER, *Eur. J. Solid State Inorg. Chem.* **26** (1989) 383.
10. E. CHRISTENSEN, J. H. VON BARNER, J. ENGELL and N. J. BJERRUM, *J. Mater. Sci.* **25** (1990) 4060.
11. I. TAOUFIK, M. HADDAD, A. NADIRI, R. BROCHU and R. BERGER, *J. Phys. Chem. Solids* **60** (1999) 701.
12. T. E. WARNER and J. MAIER, *Mat. Sci. Eng.* **B 23** (1994) 88.
13. R. J. SCHAFFER, PhD Thesis, The University of Leeds (1998).
14. A. J. DAVIDSON and D. J. FRAY, *Solid State Ionics* **136-137** (2000) 613.
15. T. E. WARNER, P. P. EDWARDS and D. J. FRAY, *Mat. Sci. Eng.* **B 8** (1991) 219.
16. R. J. SCHAFFER, R. V. KUMAR and A. E. INGHAM, *Mat. Res. Bull.* **34** (1999) 1153.
17. T. E. WARNER, W. MILIUS and J. MAIER, *Ber. Bunsenges. Phys. Chem.* **96** (1992) 1607.
18. R. AHMAMOUCHE, S. ARSALANE, M. KACIMI and M. ZIYAD, *Mat. Res. Bull.* **32** (1997) 755.
19. A. SERGHINI, R. BROCHU, R. OLAZCUAGAL and P. GRAVEREAU, *Mat. Lett.* **22** (1995) 149.

Received 14 July 2004

and accepted 25 May 2005